Table VIII. ^{13}C NMR Resonance Assignments of $(C_5HPh_4)_2Fe$ in THF and CH_2Cl_2 Solutions

resonance	assignt: carbon type	assignt: position[a]	position (ppm): THF	position (ppm): CH_2Cl_2
1	quaternary	2,5 p	135.54	133.85
2	quaternary	3,4 p	135.34	
3	ortho	3,4 p	132.41	130.52
4	ortho	2,5 p	129.44	127.65
5	meta	2,5 p	127.28	126.22
6	meta	3,4 p	126.73	125.44
7	para	2,5 p	126.13	124.87
8	para	3,4 p	126.03	
quaternary m		3,4 c	91.98	92.39
quaternary n		2,5 c	86.11	86.95
methine			b	67.24

[a] p = phenyl ring; c = cyclopentadienyl ring. [b] Obscured by solvent resonance.

^{13}C NMR spectra, the following assignments were made: resonance 3 (ortho carbon, phenyl rings 3 and 4), resonance 4 (ortho, rings 2 and 5), resonance 5 (meta, rings 2 and 5), resonance 6 (meta, rings 3 and 4), resonance 7 (para, rings 2 and 5), and resonance 8 (para, rings 3 and 4). Resonances 1 and 2 are assigned as the phenyl quaternary carbons because of their low intensity and downfield location. The $^{13}C\{^1H\}$ NMR of selectively deuterated V was required to assign these resonances. Long-range deuterium coupling resulted in only one sharp resonance for the quaternary carbon in the protiophenyl ring. Resonance 7 arises from the quaternary carbons on rings 2 and 5 and resonance 8 from those of rings 3 and 4. Low-temperature ^{13}C NMR spectra did not provide further information about the motional process.

Because of solvent overlap, assignment of the cyclopentadienyl carbons (Table VIII) was made in CH_2Cl_2 solvent. The furthest downfield resonance can be assigned to the unsubstituted carbon because of its chemical shift and high intensity. From the ^{13}C NMR spectra of III and V in THF, resonances m and n are assigned to carbons 3 and 4 and carbons 2 and 5, respectively. The detailed assignments proposed here are in substantial agreement with the those proposed for bis(diphenylcyclopentadienyl)iron(II).[34]

Acknowledgment. This material is based on work supported by the National Science Foundation (CHE-8402168 to W.C.T.). Funds supporting the purchase of the U. Delaware diffractometer were provided by NSF, and W.C.T. thanks the Alfred P. Sloan Foundation for a research fellowship. Use of the Bruker WM500 at the Southern California Regional NMR facility, supported by NSF Grant No. CHE-7916324, is acknowledged. We also thank J. M. Hanna, Jr. for helpful discussions.

Registry No. I, 15570-45-3; II, 58081-02-0; III, 12151-36-9; IV, 101200-07-1; V, 101200-08-2; Ph_4C_5O, 479-33-4.

Supplementary Material Available: Tables of structure factors, bond distances and angles, anisotropic temperature factors, and hydrogen atom coordinates (23 pages). Ordering information is given on any current masthead page.

Electron Transfer in Organometallic Clusters. 8.[1] Electron-Transfer Chain Catalyzed and Thermal Reactions of Polydentate Ligands with $RCCo_3(CO)_9$

Alison J. Downard, Brian H. Robinson,* and Jim Simpson*

Department of Chemistry, University of Otago, P.O. Box 56, Dunedin, New Zealand

Received July 18, 1985

A comparative study of the electron-transfer chain catalyzed (ETC) and thermal reactions of the polydentate ligands dppm, dppe, ttas, and tpme with $RCCo_3(CO)_9$ (R = Ph, Me) in CH_2Cl_2, THF, acetone, and CH_3CN is described. The structural types $RCCo_3(CO)_8(L\text{-}L)$, $RCCo_3(CO)_7(L\text{-}L)$ (L-L ≡ dppm, dppe), $[RCCo_3(CO)_8]_2(\mu\text{-dppe})$, $RCCo_3(CO)_6(dppm)_2$, $RCCo_3(CO)_5(dppm)_2$, $[RCCo_3(CO)_8]_2$tpme, $RCCo_3(CO)_7$tpme, and $RCCo_3(CO)_6$tpme were characterized by IR and ^1H, ^{13}C, and ^{31}P NMR spectroscopy and for $[PhCCo_3(CO)_8]_2(\mu\text{-dppe})$ by X-ray crystallography (a = 11.888 (3) Å, b = 13.059 (3) Å, c = 10.967 (1) Å, α = 97.64 (1)°, β = 118.64 (1)°, γ = 93.74 (2)°, triclinic $P\bar{1}$, Z = 1). R = 0.0405 for 3091 ($I > 3\sigma(I)$) reflections.

Electron-transfer chain catalyzed (ETC) reactions offer a rapid energy-efficient method for the activation of metal carbonyl clusters to nucleophilic substitution.[2-4] Parameters influencing the efficiency of these reactions with monodentate ligands have been delineated and include the basicity and size of the nucleophile and the kinetic stability of the intermediate cluster radical anion.[3,5] In order to study the stereochemical nuances and synthetic utility of these ETC reactions in more detail, we have turned to polydentate nucleophiles. In principle the decrease in catalytic efficiency with increasing CO substitution noted in the reactions with monodentate ligands should enable controlled selective syntheses of partially or fully ligated polydentate derivatives—an example has been given in a preliminary communication.[7] Furthermore, the $S_{RN}1$

(1) Colbran, S. B.; Robinson, B. H.; Simpson, J. *Organometallics* **1984**, *3*, 1344.

(2) Bezems, G. M.; Rieger, P. H.; Visco, S. *J. Chem. Soc., Chem. Commun.* **1981**, 265. Arewgoda, C. W.; Rieger, P. H.; Robinson, B. H.; Simpson, J.; Visco, S. *J. Am. Chem. Soc.* **1982**, *104*, 5633.

(3) Arewgoda, C. M.; Robinson, B. H.; Simpson, J. *J. Am. Chem. Soc.* **1983**, *105*, 1893.

(4) Bruce, M. I.; Hambley, T. W.; Nicholson, B. K.; Rieger, P. H.; Williams, R. L. *J. Chem. Soc., Chem. Commun.* **1982**, 442. Darchan, A.; Mahe, C.; Patin, M. *Nouv. J. Chim.* **1982**, *6*, 539; *J. Chem. Soc., Chem. Commun.* **1982**, 243. Bruce, M. I.; Matisons, J. G.; Nicholson, B. K. *J. Organomet. Chem.* **1983**, *247*, 321.

(5) Robinson, B. H.; Simpson, J.; Worth, G., submitted for publication in *J. Organomet. Chem.* Note that oxidative ETC reactions with mononuclear metal carbonyl compounds have been studied by Kochi and co-workers.[6]

(6) Hershberger, J. W.; Klinger, R. J.; Kochi, J. K. *J. Am. Chem. Soc.* **1983**, *105*, 61.

0276-7333/86/2305-1122$01.50/0

Scheme I

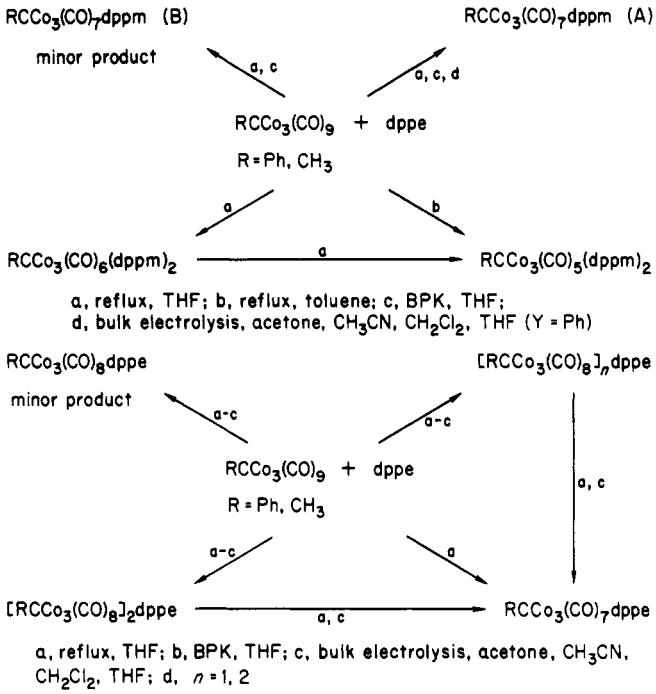

mechanism[8] imposes stereochemical constraints in carbonyl cluster systems particularly if the activated species has a "stretched" or cleaved metal–metal bond. An indication of these constraints was seen in the stereoselective synthesis of the isomers of $[(CF_3)_6C_6]Co_2(CO)_2L_2$.[9] Thus there may be opportunity to synthesize polydentate derivatives of different structural type to those accessible via thermal or photochemical methods.

These options are explored in this paper which describes the electron-initiated and thermal reactions of the bidentate ligands $Ph_2PCH_2PPh_2$ (dppm) and $Ph_2PCH_2CH_2PPh_2$ (dppe) with the tricobalt carbon clusters $RCCo_3(CO)_9$ (R = Ph, Me). A brief investigation of the reactions of $PhCCo_3(CO)_9$ with two tridentate ligands, $\{o\text{-}C_6H_4[As(CH_3)_2]\}_2AsCH_3$ (ttas) and $CH_3C(CH_2PPh_2)_3$ (tpme), is also reported. Electrochemical and mechanistic studies associated with these reactions are reported in the following papers.[10]

There is a large body of information concerning the reactions of tricobalt carbon clusters with monodentate phosphine[11-13] ligands, but at the time this work was initiated no derivatives of polydentate ligands had been reported. In the interim, Bruce et al.[4] have reported that the benzophenone ketyl (BPK) initiated reaction of $ClCCo_3(CO)_9$ with dppe afforded $ClCCo_3(CO)_7$ dppe in 50% yield, the thermal reaction of the tridentate ligand $HC(PPh_2)_3$ (TPM) with $YCCo_3(CO)_9$ (Y = H, Cl) has been shown to give $YCCo_3(CO)_7TPM$ and $YCCo_3(CO)_6TPM$,[14] and the preparation and structure of $CH_3CCo_3(CO)_7(\mu\text{-dppe})$ have been described.[15]

Scheme II

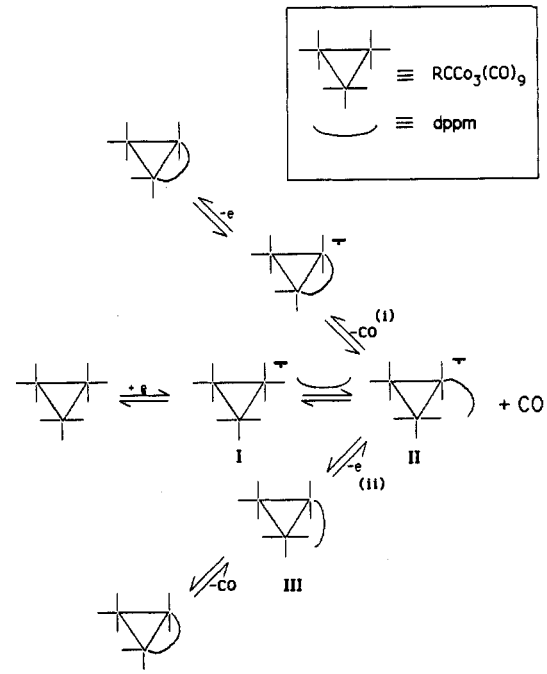

Results and Discussion

Reactions of $RCCo_3(CO)_9$ (R = Ph, CH_3) with dppm and dppe. The reactions of the clusters $RCCo_3(CO)_9$ with the potential bidentate ligands dppm and dppe gave a variety of products and yields depending on the reaction stoichiometry, reaction time, and the method of activation (thermal, BPK, or electrolytic). These results are summarized in Scheme I. In most cases, the formulation of products was supported by analytical data as well as being consistent with the IR and NMR spectral data (Table I). The following points concerning specific reactions should be noted.

Reactions with dppm. (i) The derivatives $[RCCo_3(CO)_8]_2$dppm were not identified as products in any reaction. This was unexpected since the BPK-initiated reaction of $Ru_3(CO)_{12}$ with the same ligand is reported to afford $[Ru_3(CO)_{11}]_2$dppm in 98% yield.[4]

(ii) Isomers of $RCCo_3(CO)_7(\mu\text{-dppm})$ were the only products accessible in good yield via ETC routes. These were found to be identical with clusters of the same formula isolated from thermal preparations. In all cases, formation of the major product A was accompanied by production of an isomeric complex, $RCCo_3(CO)_7(\mu\text{-dppm})$ (B), in low yield.

(iii) In addition to the formation of $PhCCo_3(CO)_7$dppm thermal reactions with excess ligand afforded the more highly substituted derivatives $PhCCo_3(CO)_6(dppm)_2$ and $RCCo_3(CO)_5(dppm)_2$ (R = Ph, CH_3). The latter clusters are the first reported tricobalt carbon derivatives of phosphorus donor ligands prepared by replacing four carbonyl groups on the parent cluster. A tetrasubstituted PMe_3 derivative has however been synthesized by Vahrenkamp by combination of metal–ligand fragments.[16] Conversion of $PhCCo_3(CO)_6(dppm)_2$ to $PhCCo_3(CO)_5(dppm)_2$ occurred rapidly in solution at ambient temper-

(7) Cunninghame, R. G.; Downard, A. J.; Hanton, L. R.; Jensen, S. D.; Robinson, B. H.; Simpson, J. *Organometallics* **1984**, *3*, 180.
(8) Bunnett, J. F. *Acc. Chem. Res.* **1978**, *11*, 413. Rossi, R. A.; Rossi, R. H. In Aromatic Substitution by the $S_{RN}1$ Mechanism; ACS Monograph 178; American Chemical Society: Washington, D.C., 1983.
(9) Arewgoda, C. M.; Robinson, B. H.; Simpson, J. *J. Chem. Soc., Chem. Commun.* **1982**, 284.
(10) (a) Downard, A. J.; Robinson, B. H.; Simpson, J. *Organometallics*, second of three papers in this issue. (b) Downard, A. J.; Robinson, B. H.; Simpson, J. *Organometallics*, third of three papers in this issue.
(11) Matheson, T. W.; Robinson, B. H.; Tham, W. S. *J. Chem. Soc. A* **1971**, 1457.
(12) Colbran, S. B.; Robinson, B. H.; Simpson, J. *Organometallics* **1983**, *2*, 952.
(13) Bruce, M. D.; Penfold, B. R.; Robinson, W. T.; Taylor, S. R. *Inorg. Chem.* **1970**, *9*, 362. Dawson, P. A.; Robinson, B. H.; Simpson, J. *J. Chem. Soc., Dalton Trans.* **1979**, 1762. Matheson, T. W.; Penfold, B. R. *Acta Crystallogr., Sect. B: Struct.* **1977**, *B33*, 1980. Penfold, B. R.; Robinson, B. H. *Acc. Chem. Res.* **1973**, *6*, 73.
(14) Maque, J. T.; Dessens, S. E. *J. Organomet. Chem.* **1984**, *262*, 347.
(15) Balavoine, G.; Collin, J.; Bonnet, J. J.; Lavigne, G. *J. Organomet. Chem.* **1985**, *280*, 429.
(16) Vahrenkamp, H., personal communication.

Table I.

IR Data[a]

	ν(CO)								
$[RCCo_3(CO)_8]_n$dppe									
R = Ph, n = 2	2078 (s)	2036 (vs)	2025 (vs)	2012 (s)	1990 (w, br)	1966 (w, br)			
R = Ph, n = 1	2078 (s) 2066 (m)	2034 (s)	2025 (vs)	2011 (s)	1990 (w, br)	1966 (w, br)			
R = Ph, n = 1	2078 (s)	2035 (vs)	2025 (vs)	2010 (s)	1986 (m, br)	1960 (w, br)			
R = CH_3, n = 2	2076 (s)	2032 (vs)	2020 (vs)	2010 (s)	1988 (m, br)	1965 (w, br)	1895 (vw, br)	1875 (w)	1850 (w, br)
R = CH_3, n = 1	2074 (m)	2030 (s)	2015 (sh)					1860 (w, br)	1825 (w, br)[b]
R = CH_3, n = 1	2076 (s)	2032 (vs)	2020 (vs)	2011 (vs)	1988 (m, br)	1962 (w)	1895 (vw, br)	1872 (w)	1850 (w, br)
$RCCo_3(CO)_7$(L–L)									
R = Ph, L–L = dppm (A)	2062 (s)	2012 (vs)	1995 (w)	1980 (w)	1973 (w)	1956 (vw, br)			
R = Ph, L–L = dppe	2060 (s)	2010 (vs)	1993 (w)	1975 (w)	1970 (w)	1950 (vw)			
R = CH_3, L–L = dppm (A)	2057 (s)	2006 (vs)	1990 (w)		1967 (w, br)	1950 (vw)			
R = CH_3, L–L = dppm (B)	2060 (s)	2007 (vw)	1993 (m)		1970 (w)	1959 (w)			
R = CH_3, L–L = dppe	2058 (s)	2008 (vs)	1989 (m)		1967 (w)	1943 (w, br)			
	2045 (w)[c]	2002 (vs)[c]					1890 (vw)	1873 (w)	1829 (w)
$RCCo_3(CO)_n(dppm)_2$									
R = Ph, n = 6[b]	2026 (sh)	2022 (s)	2017 (sh)	1985 (vs)	1985 (vs)	1907 (s, br)	1838 (w, br)	1810 (w, br)	
R = Ph, n = 5[d]	2012 (vs)	1964 (s)		1957 (s)	1930 (vw, br)	1907 (w, br)			
R = CH_3, n = 5[b]	2006 (vs)	1954 (s)			1915 (w, br)	1890 (w, br)			
$PhCCo_3(CO)_8$tpme (A)[e]	2075 (s)	2033 (vs)	2020 (vs)	2008 (s)	1985 (sh)	1960 (w)	1870 (vw)	1860 (vw)	
$PhCCo_3(CO)_7$tpme[e]	2056 (s)	2000 (vs)	1985 (sh)	1966 (w)	1937 (w)	1845 (vw)	1807 (vw)		
$PhCCo_3(CO)_6$tpme[e]	1998 (m)	1965 (vs)	1858 (w)	1818 (s)					
$PhCCo_3(CO)_6$ttas[e]	2030 (vs)	1978 (vs)	1774 (s)	1722 (m)					

NMR Data

	^1H[f]	^{31}P[g]	^{13}C[f,h]
$[PhCCo_3(CO)_8]_2$dppe	2.12, 7.04 (m)		
$[CH_3CCo_3(CO)_8]_2$dppe	2.17 (m), 2.77, 7.30 (m)	41.0	27.1 (t), 27.9 (t, J = 18), 43.1, 128.5–133.1, 205.2[j]
$CH_3CCo_3(CO)_8$dppe	2.27 (m), 2.83, 7.40 (m)	31.2 (d, J_{P-H} = 49) (*28*)[i], 40.7 (d, J_{P-H} (42) (*34*)	24.0, 29.7, 42.7, 128.4–132.4, 206.7
$PhCCo_3(CO)_7$dppe	1.97 (m), 6.88 (m), 7.32 (m)	38.7[b]	26.0 (d, t, J = 22), 125.7–132.9[j]
$CH_3CCo_3(CO)_7$dppe	2.07 (m), 3.07, 4.40 (m)		
$PhCCo_3(CO)_7$dppm	3.13 (q, J_{P-H} = 11), 3.73 (q, J_{P-H} = 11), 7.17 (m)		
$CH_3CCo_3(CO)_7$dppm (A)	3.61 (s), 3.80 (m), 7.29 (m)	35.3 (*64*)[i]	45.3 (t, t, J_{C-P} = 22), 46.0 (q), 128.3–132.0 (Ph), 205.6[j]
$CH_3CCo_3(CO)_7$dppm (B)	3.30 (s), 3.58 (m), 4.00 (m), 7.37 (m)	88.1 (*44*)[i]	128.17–130.3, 230.7
$ClCCo_3(CO)_7$dppm	3.36 (q, J_{P-H} = 12), 4.26 (q, J_{P-H} = 12), 7.22 (m)		
$PhCCo_3(CO)_5(dppm)_2$	3.00 (m), 3.82 (m), 6.90 (m)	32.6	128.6–134.4
$CH_3CCo_3(CO)_5(dppm)_2$	3.50 (m), 3.95 (m), 4.03 (s), 7.18 (m)	33.5 (*1.5*), 27.2 (*1.3*), −24.6, −30.1 (*1.0*)	

[a] Hexane, unless stated otherwise, ±1 cm^{-1}. [b] $CHCl_3$. [c] Bridged isomer. [d] CS_2. [e] CH_2Cl_2 or CD_2Cl_2. [f] ppm in $CDCl_3$, ±0.01 ppm (^1H); ppm in CD_2Cl_2, ±0.2 ppm (^{13}C); 293 K. J_{P-H} and J_{C-P} in Hz. [g] ppm (85% H_3PO_4) in CD_2Cl_2, ±0.2 ppm; singlets unless stated otherwise; italic values are the peak width at half-height; 293 K unless stated otherwise. [h] ^1H decoupled. [i] 233 K. [j] Recorded with use of INEPT techniques.

atures. The analogous CH_3CCo_3 complex, $CH_3CCo_3(CO)_6(dppm)_2$, was not detected.

A mechanistic scheme for the formation of $RCCo_3(CO)_7(\mu$-dppm) by electron-induced methods is outlined in Scheme II. Nucleophilic attack by dppm at the cluster radical anion I leads to the primary substituted cluster II. Subsequent reaction of II is via pathway i or ii. In pathway i, coordination of the second phosphorus atom occurs before electron transfer while in the alternative pathway, electron transfer occurs before coordination to leave a neutral cluster substituted by a dangling ligand which coordinates in a thermal step. In either pathway, electron transfer may be to a neutral parent cluster molecule or to the electrode (in electrolysis experiments) resulting in an electron-transfer chain reaction. Clearly the relative rates of the electron-transfer and coordination steps determine which pathway dominates, and the experimental results are consistent with either alternative; this is discussed further in a following paper.[10b]

Reactions with dppe. (i) Thermal and ETC reactions proceed via the initial formation of $[RCCo_3(CO)_8]_n$dppe (n = 1, 2) which in two cases could be isolated and characterized. Analogous complexes derived from dangling (one phosphorus atom uncoordinated) and cluster-linking ligation of dppe were also isolated by Bruce et al. from the BPK-initiated reactions of $Ru_3(CO)_{12}$ with dppe.[4]

(ii) Identical products were isolated from thermal, BPK, and electrolytic preparations.

(iii) High yields (>80%) of $RCCo_3(CO)_7(\mu$-dppe) were rapidly achieved via thermal activation while BPK-initiated reactions were slow and nonspecific. In contrast, preparations effected by bulk electrolysis proceeded cleanly in a stepwise manner to afford $PhCCo_3(CO)_7(\mu$-dppe), also in high yield.

(iv) Unlike the reactions with dppm, the success of BPK-initiated preparations of dppe derivatives were

Scheme III

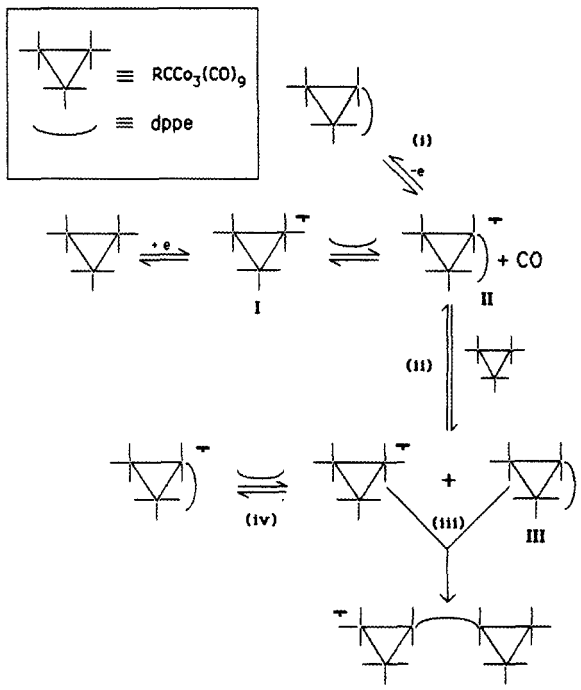

markedly dependent on the way the reactions were performed. High yields of $[RCCo_3(CO)_8]_2(\mu\text{-dppe})$ could only be achieved by using a 1:2 ligand:cluster molar ratio in dilute (10^{-2}–10^{-3} mol dm^{-3}) solutions under rigorously dry and air-free conditions. These observations are consistent with the proposed reaction mechanism shown in Scheme III.

Nucleophilic attack by dppe at the cluster radical anion I leads to the initial substituted product II. Subsequent reaction of this radical anion will be primarily via pathway i or ii. Electron transfer to adventitious oxygen or other impurities represented by step i will be favored if reaction conditions are not carefully controlled or if the concentration of substrate is low. This pathway results in formation of $RCCo_3(CO)_8$(dppe-P) and eventually $RCCo_3(CO)_7(\mu\text{-dppe})$ (via a thermal or electron-induced step). At dppe:cluster molar ratios of >1:2, pathway iv appears to compete successfully with the alternative pathway iii, again leading to monocluster complexes. Hence this mechanism predicts that the formation of the linked cluster species (which occurs via steps ii and iii will be optimized by those reaction conditions found experimentally.

Structures of dppm and dppe Derivatives of $RCCo_3(CO)_9$. There are a number of structural possibilities for these derivatives (Figure 1), and an understanding of the mode of ligand coordination in these derivatives was considered desirable prior to interpretation of their electrochemistry. IR and NMR data do not allow definitive structural assignments to be made in all cases, and so X-ray structure analyses were undertaken of complexes $CH_3CCo_3(CO)_7(\mu\text{-dppm})$ (isomer A) and $[PhCCo_3(CO)_8]_2(\mu\text{-dppe})$. The former has been recently described by Balavoine and co-workers,[15] and we will only comment on one feature not discussed by them.[17]

(i) The Crystal Structure of $CH_3CCo_3(CO)_7(\mu$-dppm). The structure of $CH_3CCo_3(CO)_7(\mu\text{-dppm})$ is derived from that of the parent cluster by replacement of two equatorial carbonyl groups on different cobalt atoms by the phosphorus atoms of the ligand. An interesting difference between the structures of $CH_3CCo_3(CO)_7(\mu\text{-dppm})$ and $CH_3CCo_3(CO)_9$ is found in the CH_3CCo_3 moiety (Figure 2). The dppm-bridged Co–Co bond is lengthened to 2.490 (3) Å compared to 2.472 (3) Å for the other Co–Co bonds. This is the expected result of the bridging requirements of the dppm ligand.[18] However, the three significantly different cobalt–apical carbon distances have no precedent in other $RCCo_3(CO)_{9-n}L_n$ derivatives. Bond lengths of 1.954 (5), 1.887 (5) and 1.82 (1) Å for the three Co–C_{ap} bonds displace the apical carbon atom toward the dppm-substituted cobalt atoms such that the carbyne ligand adopts what may be described as a semicapping orientation with respect to the cobalt triangle. It is unlikely that this distortion is steric in origin since the car-

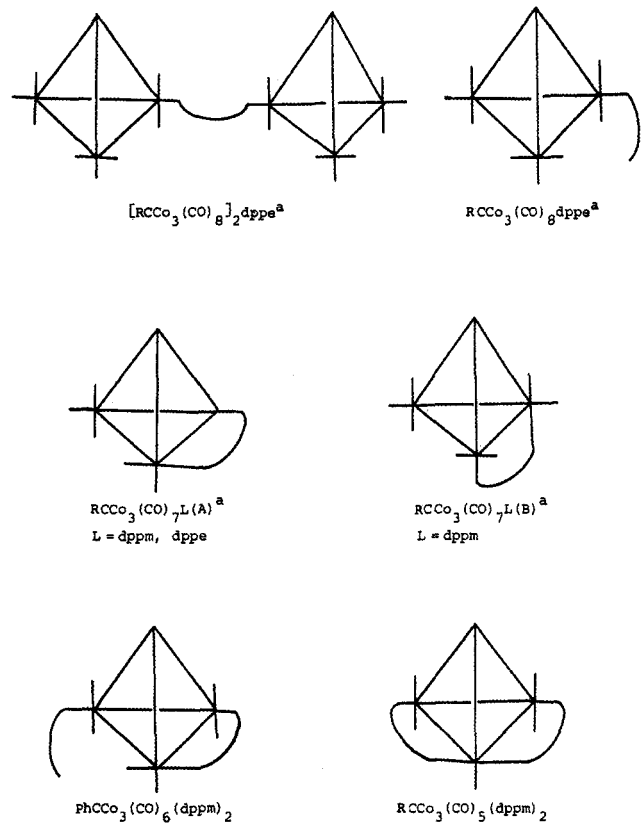

Figure 1. Structures for dppm and dppe derivatives of $RCCo_3(CO)_9$ (R = Ph, CH_3). (a) For R = CH_3, CO-bridged isomers were identified.

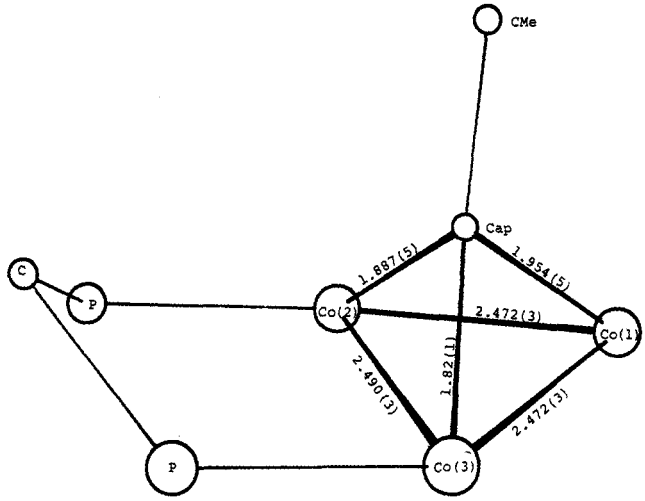

Figure 2. Cluster core geometry of the compound $CH_3CCo_3(CO)_7(\mu\text{-dppm})$.

(17) Downard, A. J. Ph.D. Thesis, University of Otago, 1984. Crystallographic data for $CH_3CCo_3(CO)_7$dppm and detailed spectroscopic data are given in the thesis.

(18) Cotton, F. A.; Troup, J. M. *J. Am. Chem. Soc.* **1974**, *96*, 4422.

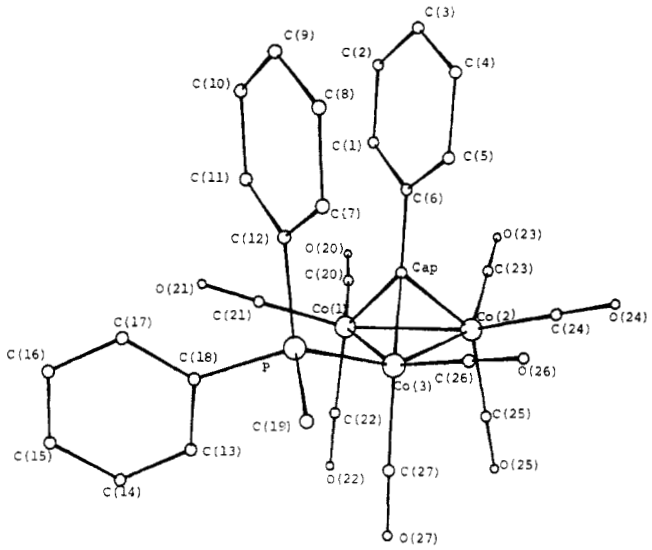

Figure 3. Structure of $[PhCCo_3(CO)_8]_2$dppe (half of the molecule only), showing the atom numbering scheme (H atoms omitted).

byne carbon atom is located closer to the sterically congested, dppm-substituted Co–Co bond. In agreement with this assertion, there is a compensatory displacement of the methyl carbon atom CMe in the direction of one Co atom.

A probable cause of the observed distortion is the buildup of electron density on the CCo_3 core as a result of dppm substitution. Di- or trisubstitution of $RCCo_3(CO)_9$ complexes by weakly π-accepting, monodentate, phosphine ligands invariably leads to the adoption of carbonyl-bridged structures with displacement of axial carbonyl ligands.[13] This allows steric relief and dissipates electron density from the cluster core by more effective $d\pi(Co) \rightarrow \pi^*(CO)$ back donation. In the present situation, carbonyl bridging is precluded by the diequatorial coordination of the dppm ligand, yet additional electron density will accrue to the CCo_3 core as a result of substitution by two relatively hard phosphine donors. An alternative mechanism for delocalization of this additional electron density would be the involvement of the appropriate carbyne p_π orbital in a localized interaction with the t_{2g} orbitals of the Co(2) and Co(3) atoms.[19] This would result in the observed displacement of the apical carbon atom toward the phosphine-substituted cobalt atoms and would also account for the observed variation in Co–C_{ap} bond lengths found in the molecule.

(ii) The Crystal Structure of $[PhCCo_3(CO)_8]_2(\mu$-dppe). $[PhCCo_3(CO)_8]_2(\mu$-dppe) crystallizes as discrete molecules. The closest intermolecular contact not involving hydrogen atoms is 3.308 Å between C(17) and C(25), indicating that the packing of these molecules is dictated by van der Waals interactions. The molecule possesses a crystallographic center of symmetry located midway between the C(19) and C(19′) atoms of the methylene groups of the dppe ligand. Figure 3, showing half of the molecule only, displays the atom labeling scheme with selected bond length and angle data given in Table II; a view of the whole molecule is given in figure 4.

The structure of $[PhCCo_3(CO)_8]_2(\mu$-dppe) is derived from that of $PhCCo_3(CO)_9$ by replacing an equatorial carbonyl group in each of the two cluster molecules by a bridging dppe ligand. The carbonyl ligands on both cluster polyhedra remain terminal as anticipated following replacement of a carbonyl from an equatorial position by the phosphine donor. Small but significant distortions in the ligand geometry have occurred on substitution as illustrated in Figure 4. It appears that, on substitution, the molecule has adopted a structure which minimizes intra-

Table II. Selected Bond Lengths and Angles for $[PhCCo_3(CO)_8]_2$dppe

Bond Lengths (Å)			
Co(1)···Co(2)	2.471 (1)	Co(3)···C(27)	1.809 (6)
Co(1)···Co(3)	2.483 (1)	C_{ap}···C(6)	1.488 (6)
C(1)···C_{ap}	1.912 (5)	P···C(12)	1.827 (4)
Co(1)···C(20)	1.781 (6)	P···C(18)	1.830 (4)
Co(1)···C(21)	1.776 (7)	P···C(19)	1.839 (5)
Co(1)···C(22)	1.796 (7)	C(19)···C(19)	1.57 (1)
Co(2)···Co(3)	2.479 (1)	C(20)···O(20)	1.142 (7)
Co(2)···C_{ap}	1.932 (5)	C(21)···O(21)	1.142 (7)
Co(2)···C(23)	1.807 (7)	C(22)···O(22)	1.150 (7)
Co(2)···C(24)	1.784 (8)	C(23)···O(23)	1.118 (7)
Co(2)···C(25)	1.822 (7)	C(24)···O(24)	1.126 (8)
Co(3)···C_{ap}	1.887 (5)	C(25)···O(25)	1.133 (7)
Co(3)···P	2.229 (1)	C(26)···O(26)	1.144 (7)
Co(3)···C(26)	1.761 (6)	C(27)···O(27)	1.141 (6)
Bond Angles (deg)			
Co(2)–Co(1)–Co(3)	60.10 (1)	Co(2)–Co(3)–P	155.70 (1)
Co(2)–Co(1)–C_{ap}	50.4 (1)	Co(2)–Co(3)–C(26)	95.9 (2)
Co(2)–Co(1)–C(20)	96.8 (2)	Co(2)–Co(3)–C(27)	101.5 (2)
Co(2)–Co(1)–C(21)	153.7 (2)	C_{ap}–Co(3)–P	105.5 (1)
Co(2)–Co(1)–C(22)	98.7 (2)	C_{ap}–Co(3)–C(26)	104.6 (2)
Co(3)–Co(1)–C_{ap}	48.8 (1)	C_{ap}–Co(3)–C(27)	144.0 (2)
Co(3)–Co(1)–C(20)	153.1 (2)	P–Co(3)–C(26)	91.4 (2)
Co(3)–Co(1)–C(21)	101.9 (2)	P–Co(3)–C(27)	100.0 (2)
Co(3)–Co(1)–C(22)	95.8 (2)	C(26)–Co(3)–C(27)	99.8 (3)
C_{ap}–Co(1)–C(20)	106.7 (2)	Co(1)–C_{ap}–Co(2)	80.0 (2)
C_{ap}–Co(1)–C(21)	103.5 (2)	Co(1)–C_{ap}–Co(3)	81.6 (2)
C_{ap}–Co(1)–C(22)	139.6 (3)	Co(2)–C_{ap}–Co(3)	80.9 (2)
C(20)–Co(1)–C(21)	94.3 (3)	Co(1)–C_{ap}–C(6)	132.8 (3)
C(20)–Co(1)–C(22)	101.6 (3)	Co(2)–C_{ap}–C(6)	126.1 (3)
C(21)–Co(1)–C(22)	102.3 (3)	Co(3)–C_{ap}–C(6)	135.1 (3)
Co(1)–Co(2)–Co(3)	60.20 (1)	C_{ap}–C(6)–C(1)	120.1 (2)
Co(1)–Co(2)–C_{ap}	49.6 (1)	C_{ap}–C(6)–C(5)	119.9 (2)
Co(1)–Co(2)–C(23)	97.3 (2)	Co(3)–P–C(12)	115.1 (1)
Co(1)–Co(2)–C(24)	152.3 (2)	Co(3)–P–C(18)	120.1 (1)
Co(1)–Co(2)–C(25)	98.8 (2)	Co(3)–P–C(19)	109.4 (2)
Co(3)–Co(2)–C_{ap}	48.7 (1)	C(12)–P–C(18)	106.1 (2)
Co(3)–Co(2)–C(23)	148.8 (2)	C(12)–P–C(19)	104.0 (2)
Co(3)–Co(2)–C(24)	97.2 (2)	C(18)–P–C(19)	100.0 (2)
Co(3)–Co(2)–C(25)	99.6 (2)	P–C(12)–C(7)	120.1 (1)
C_{ap}–Co(2)–C(23)	100.6 (2)	P–C(12)–C(11)	119.8 (1)
C_{ap}–Co(2)–C(24)	104.0 (3)	P–C(18)–C(13)	117.3 (1)
C_{ap}–Co(2)–C(25)	141.5 (3)	P–C(18)–C(17)	122.1 (1)
C(23)–Co(2)–C(24)	96.1 (3)	P–C(19)–C(191)	114.3 (4)
C(23)–Co(2)–C(25)	105.5 (3)	Co(1)–C(20)–O(20)	177.0 (6)
C(24)–Co(2)–C(25)	100.8 (3)	Co(1)–C(21)–O(21)	175.4 (5)
Co(1)–Co(3)–Co(2)	59.70 (1)	Co(1)–C(22)–O(22)	178.7 (8)
Co(1)–Co(3)–C_{ap}	49.6 (1)	Co(2)–C(23)–O(23)	178.6 (6)
Co(1)–Co(3)–P	105.70 (1)	Co(2)–C(24)–O(24)	178.3 (6)
Co(1)–Co(3)–C(26)	151.7 (2)	Co(2)–C(25)–O(25)	178.8 (6)
Co(1)–Co(3)–C(27)	99.2 (2)	Co(3)–C(26)–O(26)	179.0 (6)
Co(2)–Co(3)–C_{ap}	50.3 (1)	Co(3)–C(27)–O(27)	177.7 (5)

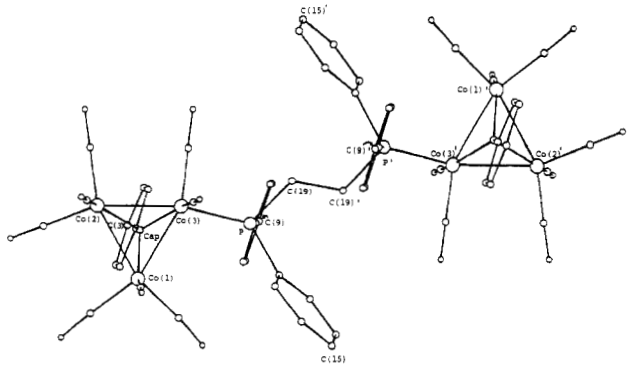

Figure 4. View of $[PhCCo_3(CO)_8]_2$dppe perpendicular to the Co_3 triangles.

(19) Schilling, B. E. R.; Hoffmann, R. *J. Am. Chem. Soc.* **1978**, *100*, 6274. Kostic, N. M.; Fenske, R. F. *J. Am. Chem. Soc.* **1982**, *104*, 3879.

molecular interactions between the phenyl rings of the dppe ligand and both the phenyl substituent of the carbyne ligand and the ligated carbonyl groups. Thus the apical phenyl ring (C(1)–C(6)) and one of the phenyl substituents of the phosphine ligand (C(7)–C(12)) lie almost parallel, maximizing the nonbonded distances between the ring carbon atoms; the angle between the two least squares ring planes is 7.4°. This orientation is achieved by tilting the C_{ap}–C(6) bond toward Co(2) such that the angle T_c–C_{ap}–C(6) is 173.5° (T_c is the centroid of the cobalt triangle); the plane of the apical phenyl ring is inclined at 84.4° to the plane of the cobalt triangle. Similarly, angles of 105.7 (1) and 101.9 (2)° for Co(1)–Co(3)–P and Co(3)–Co(1)–C(21), respectively, are considerably larger than the corresponding angles between the carbonyl ligands in $CH_3CCo_3(CO)_9$ or $PhCCo_3(CO)_9$.[20] This widening helps to achieve the parallel ring configuration and, at the same time, reduces steric interactions between the equatorial carbonyl group C(21)–O(21) and the atoms of the C(13)–C(18) ring.

Bending of Co–P bonds toward the Co_3 plane was observed for $CH_3CCo_3(CO)_8PPh_3$ and $CH_3CCo_3(CO)_6[P(OMe)_3]_3$[13] with C_{ap}–Co–P angles in the range 111–113°. However in this derivative, the C_{ap}–Co(3)–P angle is reduced to 105.5 (1)°, reflecting the effectiveness of the parallel ring orientation in minimizing nonbonded contacts between the apical phenyl substituent and the phosphine ligand. The geometry of the CCo_3 moiety and the orientation of the axial carbonyl ligands are essentially the same as those found for $CH_3CCo_3(CO)_9$ and $PhCCo_3(CO)_9$[20] apart from a small but anticipated[13] lengthening of the Co–Co bonds; all other bond lengths and angles are unremarkable.

(iii) The Solution Structures of dppm Derivatives. NMR and IR data for $RCCo_3(CO)_7$dppm (A) (Table I) are consistent with the solid-state structure[15] of $CH_3CCo_3(CO)_7(\mu$-dppm) (structural type A, Figure 1), indicating that no structural change occurs on dissolution. ^1H NMR spectra indicate nonequivalence of the methylene protons of the bridging ligand. This is expected since the geometry of the molecule leads to chemically different environments for the two protons. The ^{31}P chemical shift of 35.3 ppm is similar to those reported for $Co_4(CO)_8$dppm and $Co_4(CO)_6$(dppm)$_2$ (30.4 and 25.94 ppm, respectively) where the ligand is also presumed to adopt a Co–Co bond bridging coordination.[21]

The other isomer of $RCCo_3(CO)_7(\mu$-dppm) can be assigned to structure B in Figure 1. It has been proposed that the mode of coordination (chelating vs. bridging) of multidentate phosphine ligands can be determined from ^{31}P chemical shifts.[22] In particular the formation of a four-membered chelate ring with dppm results in a considerable upfield shift of the ^{31}P resonance compared to that observed when the ligand is monodentate or bridging two metals. By these arguments the shift downfield observed for $CH_3CCo_3(CO)_7$dppm (B) (δ 88.1) is inconsistent with a structure with a chelating dppm on one cobalt atom. Moreover the ligated phosphorus atoms of an alternative equatorial/axial configuration would be stereochemically inequivalent, but there is no evidence of magnetic inequivalence in the ^{31}P NMR spectrum. While the lack of signal resolution could account for this, structure B is nevertheless preferred since axial/equatorial substitution of carbonyl groups within the same molecule has not been observed for tricobalt carbon clusters.[13]

Numerous structures incorporating chelating and bridging dppm ligands can be proposed for complexes of formula $RCCo_3(CO)_5$(dppm)$_2$. The ^{31}P spectrum of $PhCCo_3(CO)_5$(dppm)$_2$ exhibits one broad signal (ν_1 = 70 Hz) at 32.6 ppm, indicating that a structure involving chelation of dppm is unlikely. Bridging ν(CO) bands are not observed which leaves five possible structures. Stereochemically inequivalent phosphorus atoms are required by all structures, and presumably the lack of signal resolution prevents detection of magnetic inequivalence. The structure in Figure 1 is preferred since only this mode of coordination results in stereochemically equivalent environments for the methylene protons on each ligand (giving rise to two types of ^1H in the molecule) which is consistent with the ^1H NMR spectrum.

The ^{31}P NMR spectrum of $CH_3CCo_3(CO)_5$(dppm)$_2$ is more complex. The approximate relative intensity of signals at 33.5, 27.2, and −30.1 ppm is 6:2; the weak signal at −24.6 ppm is assigned to free dppm. A chemical shift of −30.1 ppm is within the range of values reported for both the uncoordinated phosphorus of a dangling ligand and the phosphorus incorporated in a four-membered ring, while the downfield signals are indicative of bridging of a Co–Co bond by the ligand or coordination of one phosphorus of a dangling ligand.[22] We suggest that $CH_3CCo_3(CO)_5$(dppm)$_2$ exists mainly in the same form as $PhCCo_3(CO)_5$(dppm)$_2$, giving rise to the signal at 33.5 ppm. A second species present in solution has one of two possible structures: an isomer in which one ligand bridges a Co–Co bond and the other chelates to the third cobalt for (δ 27.2 and −30.1), or alternatively a molecule in which one dppm bridges a Co–Co bond (δ 33.5) and the other coordinates in a dangling fashion (δ_{coord} 27.2 and $\delta_{uncoord}$ −30.1).

The structure of $PhCCo_3(CO)_6$(dppm)$_2$ is most probably based on that of $PhCCo_3(CO)_5$(dppm)$_2$ discussed above, where each cobalt atom is equatorially substituted by one phosphorus atom leaving one pendant dppm ligand. The lability of this complex did not allow collection of NMR data.

(iv) The Solution Structures of dppe Derivatives. The energy of the A_1 ν(CO) mode and the spectral profiles of *three* derivatives (Table I) are identical with those reported for $RCCo_3(CO)_8PPh_3$ (R = Ph, CH_3),[11,12] indicating the coordination of one phosphorus atom per dppe per cluster. Spectroscopic data for $[PhCCo_3(CO)_8]_2(\mu$-dppe) suggest that its solution structure is the same as that revealed by X-ray analysis. However, IR data for the methyl cluster analogue (the high yield, stable product) show weak bands due to bridging carbonyls in both the solid and the solution, presumably indicating a mixture of carbonyl-bridged and nonbridged isomers. Similar behavior has been noted for $CH_3CCo_3(CO)_8L$ derivatives in solution.[11]

NMR data for a second stable derivative confirms its formulation as $RCCo_3(CO)_8$(dppe-P). Thus the ^{31}P NMR spectrum of $CH_3CCo_3(CO)_8$dppe consists of two doublets centred at 40.7 and 31.2 ppm corresponding to the coordinated and uncoordinated phosphorus atoms, respectively. Again weak bridging carbonyl bands are seen in the solution IR of the methyl but not the phenyl cluster derivative. Equatorial substitution by a phosphorus atom is most probable for the nonbridged clusters while $CH_3CCo_3(CO)_8$dppe presumably also exists in an axially substituted, carbonyl-bridged conformation (as found for $CH_3CCo_3(CO)_8P(C_6H_{11})_3$, for example[11]).

The instability of the third derivative described as $[RCCo_3(CO)_8]_n$(dppe)$_m$ prevented further characterization.

(20) Sutton, P. W.; Dahl, L. F. *J. Am. Chem. Soc.* **1967**, *89*, 262; Colbran, S. B.; Robinson, B. H., Simpson, J. *Acta Crystallogr.* in press.
(21) Rimmelin, J.; Lemonine, P.; Gross, M. *Nouv. J. Chim.* **1983**, *7*, 453.
(22) Garrout, P. E. *Chem. Rev.* **1981**, *81*, 229.

The spectroscopic data for $PhCCo_3(CO)_7$dppe is consistent with a structure analogous to that of $RCCo_3(CO)_7(\mu$-dppm). $CH_3CCo_3(CO)_7(\mu$-dppe) exists in both carbonyl-bridged and nonbridged configurations which presumably corresponds to diaxial and diequatorial substitution by dppe, respectively.

Reactions of $PhCCo_3(CO)_9$ with ttas and tpme. The reactions of $PhCCo_3(CO)_9$ with the potential tridentate ligands ttas and tpme indicated that a large number of substituted cluster derivatives were accessible, particularly by electron-induced methods (see Experimental Section).

The BPK-induced reaction with ttas led to the almost simultaneous formation of at least six products while with tpme the reaction afforded derivatives in which one or two carbonyl groups had been replaced by phosphorus atoms. Bulk electrolysis in CH_3CN enabled the selective preparation of octacarbonyl derivatives and ligation of a second phosphorus atom was achieved in a second controlled step. In refluxing THF, a rapid reaction afforded $PhCCo_3(CO)_6(\mu$-tpme) as the major product but decomposition occurred with ttas.

The structure of $PhCCo_3(CO)_6(\mu$-tpme) most likely involves triaxial coordination by the tridentate ligand similar to that in $ClCCo_3(CO)_6$TPM.[14] The more flexible bite of the tpme ligand might permit other modes of coordination, but the triaxial structure has also been suggested for $RCCo_3(CO)_6L_3$ which shows evidence of bridging carbonyl groups.[11] The $\nu(CO)_{t\text{-}sym}$ mode of $PhCCo_3(CO)_6(\mu$-tpme) is of similar energy to that of $PhCCo_3(CO)_6(Et_2PhP)_3$,[11] and the spectral profile matches that of $FcCCo_3(CO)_6L_3$.[12]

The structure of $PhCCo_3(CO)_6$ttas poses a more interesting problem since IR data suggest a triply bridging carbonyl group ($\nu(CO) = 1722$ cm^{-1}). Chelation of all arsenic donor atoms to single cobalt atom with a concomitant molecular rearrangement to afford a semibridging carbonyl group was observed in $(CF_3)_2C_2Co_2(CO)_3$ttas.[7] Similar coordination of the tridentate ligand in $PhCCo_3(CO)_6$ttas could also be accompanied by rearrangement of the carbonyl ligand geometry. Alternatively, coordination of two arsenic atoms to one cobalt and a bridge to a second metal atom might also cause a sufficiently asymmetric electron density distribution to necessitate the formation of a triply bridging carbonyl.

Conclusion

Preparation of dppm, dppe, and tpme derivatives of clusters $RCCo_3(CO)_9$ by electron-induced methods offers no net advantage over the traditional thermal methods. This is mainly because thermal preparations of these derivatives are rapid and easily controlled. Highly substituted derivatives are only accessible in good yield from thermal reactions, while electron-induced methods provide a more convenient route to the partially ligated derivatives $[RCCo_3(CO)_8]_2$dppe and $RCCo_3(CO)_n$tpme (n = 7, 8). Nevertheless, this work established that these clusters readily undergo ETC reactions and that a closer study by transient electrochemical techniques was warranted.

Experimental Section

Synthetic Procedures. The clusters $ClCCo_3(CO)_9$, $CH_3CCo_3(CO)_9$, and $PhCCo_3(CO)_9$ were prepared according to published procedures from the reaction of dicobalt octacarbonyl (Aldrich) with the corresponding α,α',α''-trihalide YCX_3.[23] Bis(diphenylphosphino)methane (dppm), bis(1,2-diphenylphosphino)ethane (dppe), and 1,1,1-tris((diphenylphosphino)methyl)ethane (tpme) (Strem) were used without purification. Bis(*o*-(dimethylarsino)phenyl)methylarsine (ttas) was prepared by the literature procedure[24] by Dr. R. G. Cunninghame (University of Otago). Solvents were dried and purified as outlined previously.[3] Analytical thin-layer chromatography (TLC) and solution infrared (ν(CO) region) were used to monitor reactions. Separation of reaction products by preparative TLC was often difficult due to the similar R_f values of the products, and several platings were sometimes required to yield the pure compound. Analytical data are given in the deposited material.

Bulk electrolysis reactions were performed in a standard three-electrode cell. Typically 20 or 30 cm^3 of 0.1 mol dm^{-3} supporting electrolyte solution was used. Unless otherwise stated, Et_4NClO_4 was used as supporting electrolyte in CH_3CN and acetone, while Bu_4NClO_4 was used for electrolysis experiments in CH_2Cl_2 and THF. Stirring of the electrolysis solution was achieved by bubbling argon or nitrogen through the solution during the reaction. The reactions were monitored by analysis of samples withdrawn from the cell by syringe. Two methods were used to recover the reaction products from the electrolyte solutions. After removal of the solvent under reduced pressure, residues containing Bu_4NClO_4 were dissolved in a small volume of THF and hexane was added to precipitate the electrolyte which was then removed by filtration. Residues containing Et_4NClO_4 were dissolved in CH_3CN and the products repeatedly extracted into hexane. When the reaction products were extremely air sensitive (especially radical anions), the whole electrolysis apparatus was enclosed in a plastic bag continually flushed with Ar. Samples for IR and TLC analysis could then be withdrawn through the plastic bag with an air-tight syringe to maintain anaerobic conditions. This simple setup gave an ease of access which is difficult in an Ar atmosphere drybox.

Preparation of Benzophenone Ketyl (BPK). To 15 cm^3 of dry degassed THF in a two-neck flask was added finely cut sodium (~0.5 cm^3). This was stirred under an inert atmosphere for ~60 min. Benzophenone (0.07 g, 0.37 mmol) was added and the solution stirred at room temperature until a deep purple color developed (~60 min). This gave a solution of $\sim 2.5 \times 10^{-2}$ mol dm^{-3} BPK. The inert atmosphere was maintained as aliquots were withdrawn with an argon- or nitrogen-flushed syringe, and with careful treatment the solution could be used for several months.

Preparation of $PhCCo_3(CO)_7$dppm (A and B) and $PhCCo_3(CO)_5(dppm)_2$. (a) Thermal Reaction. $PhCCo_3(CO)_9$ (0.10 g, 0.2 mmol) and dppm (0.15 g, 0.4 mmol) were heated to reflux for 15 min in 20 cm^3 of THF. The mixture was cooled, the solvent was removed under reduced pressure, and the crude products were subjected to preparative TLC (silica gel plates). Development in $CHCl_3$/hexane (1:2) partially separated seven bands. After several elutions, a separation was achieved and the products were removed with $CHCl_3$ to yield: band 1, unreacted $PhCCo_3(CO)_9$ (10%), red-brown; band 2, $PhCCo_3(CO)_7$dppm (A) (55%), brown; band 3, $PhCCo_3(CO)_6(dppm)_2$ (20%), green; band 4, $PhCCo_3(CO)_5(dppm)_2$ (10%), yellow-brown; band 5, $PhCCo_3(CO)_7$dppm (B), red-brown. The remaining products were not recovered in sufficient amounts to allow characterization. $PhCCo_3(CO)_7$dppm (A) was readily crystallized from $CHCl_3$/ethanol. $PhCCo_3(CO)_6(dppm)_2$ was unstable in the solid and in solution at 0 °C and gradually converted to $PhCCo_3(CO)_5(dppm)_2$ and $PhCCo_3(CO)_7$dppm. Numerous attempts to crystallize $PhCCo_3(CO)_6(dppm)_2$ were unsuccessful.

In an attempt to improve the yield of $PhCCo_3(CO)_7$dppm (A) the reaction was repeated by using both a 3 molar excess of the ligand and an equimolar amount, but this made little difference to the yield of the desired product. The reaction was also carried out in hexane, but this favoured the formation of the more highly substituted derivatives.

(b) ETC Reactions. (i) Using BPK. $PhCCo_3(CO)_9$ (0.10 g, 0.2 mmol) and dppm (0.08 g, 0.22 mmol) were dissolved in 20 cm^3 of dry degassed THF in a two-neck 25-cm^3 flask. BPK ($\sim 2.5 \times 10^{-2}$ mol dm^{-3}) was added dropwise to the stirred solution until no parent cluster remained. The volume of BPK required depended on the dryness of the solvent and the inert atmosphere

(23) Seyferth, D.; Hallgren, J. E.; Hung, P. L. K. *J. Organomet. Chem.* **1973**, *50*, 265.

(24) Cunninghame, R. G.; Nyholm, R. S.; Tobe, M. C. *J. Chem. Soc.* **1964**, 5800.

used. Air was admitted to the flask, and the solvent was removed under reduced pressure at room temperature. Chromatography using silica gel plates and 1:2 $CHCl_3$/hexane separated the major dark brown band ($R_f \sim 0.4$) from a number of very faint green and brown bands with $R_f < 0.4$. Removal of the major product with $CHCl_3$ yielded $PhCCo_3(CO)_7$dppm (A) (0.12 g, 0.14 mmol, 70%).

(ii) Bulk Electrolysis. High-yield preparations of $PhCCo_3(CO)_7$dppm (A) could be carried out in all four solvents investigated: acetone, CH_3CN, CH_2Cl_2, and THF.

In a typical preparation, dppm (0.09 g, 0.23 mmol) was dissolved in 20 cm^3 of degassed solvent (0.1 mol dm^{-3} supporting electrolyte). The solution was electrolyzed at the reduction potential of $PhCCo_3(CO)_9$ until the current decayed to a constant value. $PhCCo_3(CO)_9$ (0.10 g, 0.2 mmol) was added and the solution electrolyzed at the same potential until the current again decayed to the background value. Analytical TLC and IR of the resulting solutions showed that for all solvents used, <5% of the cluster remained unreacted and conversion to $PhCCo_3(CO)_7$dppm (A) was >90%.

Preparation of $PhCCo_3(CO)_5(dppm)_2$. This derivative was only accessible in good yield by thermal synthesis. The most convenient preparation was to reflux $PhCCo_3(CO)_9$ (0.05 g, 0.1 mmol) and dppm (0.11 g, 0.3 mmol) in 10 cm^3 of toluene for 10 min. The solvent was removed and the residue dissolved in $CHCl_3$. Material that was insoluble in $CHCl_3$ was discarded. Chromatography on silica gel plates and development in $CHCl_3$/hexane (1:2) separated the product (yellow brown band, $R_f \sim 0.2$) from excess dppm; crystallization from $CHCl_3$/ethanol gave $PhCCo_3(CO)_5(dppm)_2$ (0.06 g, 0.05 mmol, 55% yield) as microcrystals.

Preparation of $CH_3CCo_3(CO)_7$dppm Isomers A and B. (a) Thermal Reaction. The procedure was the same as that given for the preparation of the analogous phenyl cluster derivatives. Reflux of $CH_3CCo_3(CO)_9$ (0.09 g, 0.2 mmol) and dppm (0.15 g, 0.4 mmol) in 20 cm^3 of THF for 15 min was followed by chromatographic separation on silica gel plates. Elution with acetone/hexane (1:2) separated five bands. Products were removed with acetone to yield: band 1, $CH_3CCo_3(CO)_7$dppm (A) (83%), purple-brown; band 2, $CH_3CCo_3(CO)_7$dppm (B) (5%) purple; band 3, $CH_3CCo_3(CO)_5(dppm)_2$ (1%), yellow-brown. Insufficient material was recovered from bands 4 and 5 to allow further characterization. $CH_3CCo_3(CO)_7$dppm (A) was crystallized from $CHCl_3$/ethanol or from hot hexane.

(b) BPK Reaction. $CH_3CCo_3(CO)_9$ (0.09 g, 0.2 mmol) and dppm (0.08 g, 0.22 mmol) were dissolved in 20 cm^3 of dry, degassed THF in a two-neck 25-cm^3 flask. BPK ($\sim 2.5 \times 10^{-2}$ mol dm^{-3}) was added dropwise to the stirred solution until all parent cluster had been consumed. Air was admitted to the flask, and the solvent was removed under reduced pressure at room temperature. Chromatography using silica gel plates and 1:2 acetone/hexane separated five bands. Products were removed with acetone to yield: band 1, $CH_3CCo_3(CO)_7$dppm (A) (83%); band 2, $CH_3CCo_3(CO)_7$dppm (B) (10%). The remaining products were not recovered in sufficient amounts to allow characterization.

Preparation of $CH_3CCo_3(CO)_5(dppm)_2$. $CH_3CCo_3(CO)_9$ (0.045 g, 0.1 mmol) and dppm (0.12 g, 0.3 mmol) were gently refluxed in toluene for ~30 min. The solution was cooled and filtered and the crude product chromatographed on silica gel plates. Development in CH_2Cl_2/hexane (6:1) separated the major yellow band ($R_f \sim 0.8$) from a faint purple brown band ($R_f \sim 0.9$) and from a substantial amount of insoluble brown material (R_f 0). The yellow brown band gave $CH_3CCo_3(CO)_5(dppm)_2$ (0.09 g, 0.08 mmol, 80% yield). The IR spectrum of the purple brown band identified it as $CH_3CCo_3(CO)_7$dppm. A similar yield of $CH_3CCo_3(CO)_5(dppm)_2$ was achieved by stirring the reactants in toluene at 100 °C.

Preparation of $[PhCCo_3(CO)_8]_2$dppe. ETC reactions were found to offer the best route to this derivative. Yields from BPK initiated reactions were markedly dependent on the concentration used and the dryness of the THF, but with a concentration of cluster >6×10^{-3} mol dm^{-3} and rigorously dried and degassed solvent, isolated yields of >80% could be achieved.

Typically, $PhCCo_3(CO)_9$ (0.036 g, 0.07 mmol) and dppe (0.014 g, 0.035 mmol) were stirred in 10 cm^3 of THF. BPK was added dropwise until only a trace of cluster remained unreacted. The solvent was removed and the residue chromatographed on silica gel plates. Elution with acetone/hexane (1:2) separated a dark brown band ($R_f \sim 0.6$) from a number of very faint bands with small R_f values. The product from the major band was crystallized from $CHCl_3$/ethanol to give $[PhCCo_3(CO)_8]_2$dppe (0.04 g, 0.03 mmol, 83% yield).

Preparation of $PhCCo_3(CO)_7$dppe. BPK-initiated reactions of $PhCCo_3(CO)_9$ and dppe initially produced monosubstituted derivatives, but on addition of more BPK, $PhCCo_3(CO)_7$dppe was produced as well as a number of other products. The difficulty of purifying the desired product (which formed in ~50% yield) and the considerable amount of decomposition to noncluster species which occurred in these reactions made other preparative routes more attractive.

(a) Thermal Reaction. $PhCCo_3(CO)_9$ (0.05 g, 0.1 mmol) and dppe (0.04 g, 0.1 mmol) were refluxed for ~5 min in 10 cm^3 of THF. The solution was cooled, the solvent was removed under reduced pressure, and the residue was chromatographed on silica gel plates. Development in $CHCl_3$/hexane (1:2) separated a dark yellow brown band ($R_f \sim 0.3$) from several bands with smaller R_f values. Crystallization of the major product from $CHCl_3$/ethanol gave $PhCCo_3(CO)_7$dppe (0.07 g, 0.08 mmol, 80% yield).

(b) Bulk Electrolysis. Acetone, CH_3CN, CH_2Cl_2, and THF were all suitable solvents for the preparation of $PhCCo_3(CO)_7$dppe. Typically, dppe (0.09 g, 0.23 mmol) was dissolved in 20 cm^3 of solvent (0.1 mol dm^{-3} supporting electrolyte) using an ultrasonic bath if necessary. The solution was degassed and preelectrolyzed at the reduction potential of the parent cluster until a steady background current was reached. $PhCCo_3(CO)_9$ (0.10 g, 0.2 mmol) was added and the electrolysis continued at the same potential until the current again fell near to the background value and TLC analysis showed almost complete conversion to $PhCCo_3(CO)_8$ dppe, $[PhCCo_3(CO)_8]_n(dppe)_m$, and $[PhCCo_3(CO)_8]_2$dppe. The potential was then made ~0.2 V more negative which resulted in an increase of current. The fall-off of the current was less rapid for this step, but when a steady value was again reached, TLC and IR analysis showed >80% conversion to $PhCCo_3(CO)_7$dppe.

Preparations of Other dppe Derivatives of $PhCCo_3(CO)_9$. Attempts were made to maximize the yields of several other products formed in small amounts in the preparations described above.

$[PhCCo_3(CO)_8]_n$dppe (n = 1, 2). Reactions of $PhCCo_3(CO)_9$ with dppe always resulted in the formation of a dark brown product with an R_f value greater than that of $[PhCCo_3(CO)_8]_2$dppe. This product formed in high yield during the initial stages of thermal and ETC substitution but rapidly underwent further reaction to yield the thermodynamically favored products. The best method for the preparation of this compound was by a BPK-initiated reaction at 0 °C which slowed down formation of $PhCCo_3(CO)_7$dppe.

Typically, $PhCCo_3(CO)_9$ (0.02 g, 0.035 mmol) and dppe (0.05 g, 0.12 mmol) were dissolved in 4 cm^3 of THF. The solution was cooled to 0 °C and BPK added dropwise until all parent cluster had been consumed. The solvent was removed at 0 °C and the residue chromatographed on silica gel plates and developed in acetone/hexane (1:2). A dark brown band ($R_f \sim 0.8$) separated cleanly from a second brown band ($R_f \sim 0.6$, identified as $[PhCCo_3(CO)_8]_2$dppe) and several other faint bands with smaller R_f values. The major product was washed from the gel with acetone and dried to give 0.027 g of a dark solid. Analytical TLC of this material dissolved in CH_2Cl_2 showed a mixture of equal amounts of the required product $PhCCo_3(CO)_7$dppe and $PhCCo_3(CO)_8$dppe. An IR spectrum of the CH_2Cl_2 solution showed peaks corresponding to $PhCCo_3(CO)_7$dppe and $[PhCCo_3(CO)_8]_n$dppe only. Due to the facile conversion of $PhCCo_3(CO)_8$dppe into other species, further characterization of this product was not attempted.

Preparation of $PhCCo_3(CO)_8$dppe. A third brown product with an IR spectrum typical of a monophosphine-substituted cluster ($R_f \sim 0.3$; acetone/hexane, 1:2) was produced in low yields in these preparations. Attempts were made to achieve a higher yield of this product by varying the conditions of thermal and BPK reactions in the following ways: the molar ratio of dppe: cluster was varied from 1:2 to 2:1; BPK reactions were performed at 0 °C and at room temperature, and small and relatively large amounts of BPK were added. In addition, preparations were

Table III. Crystal Data, Data Collection, and Refinement of $[PhCCo_3(CO)_8]_2dppe$

Crystal Data for $[PhCCo_3(CO)_8]_2dppe$
crystal system: triclinic
a = 11.888 (3) Å
b = 13.059 (3) Å
c = 10.967 (2) Å
α = 97.64 (1)°
β = 118.64 (1)°
γ = 93.74 (2)°
V = 1464.6 Å^3
formula: $C_{56}H_{34}O_{16}P_2Co_6$
fw: 1378.43 g mol^{-1}
D_{calcd} = 1.56 g cm^{-3}
Z = 1
$F(000)$ = 689.94
cryst size: 0.45 × 1.4 × 1.5 mm
μ(Mo Kα) = 16.96 cm^{-1}

Data Collection and Refinement for $[PhCCo_3(CO)_8]_2dppe$
diffractometer: Nicolet P$\bar{3}$
radiation: Mo Kα (λ = 0.710 69 Å)
scan type: θ–2θ
data limits: $0 < 2\theta < 45°$
reflctns measd: $\pm h,k,l$
cryst decay: <2%[a]
total obsd data: 3846
unique data: 3091 ($I > 3\sigma(I)$)
abs correctn: empirical[b]
max transmissn: 0.680
minimum transmissn: 0.580
no. of variables: 263
$R(\sum||F_o| - |F_c||/|F_o|) = 0.0405$
$R_w[\sum w^{1/2}||F_o| - |F_c||/\sum w^{1/2}|] = 0.0448$
$w = [2.458/(\sigma^2(F) + 0.00\,419F^2)]$

[a] Standard reflections (7, 2, −1), (0, 5, −6), and (1, 9, −1) measured after every 50 reflections. [b] See ref 25.

attempted by heating, electrolyzing, or adding BPK to solutions of $[PhCCo_3(CO)_8]_2dppe$, but in no case was a yield of >10% achieved.

Preparation of $[CH_3CCo_3(CO)_8]_2dppe$. $CH_3CCo_3(CO)_9$ (0.18 g, 0.4 mmol) and dppe (0.08 g, 0.2 mmol) were dissolved in 20 cm^3 of THF. BPK was added dropwise until TLC showed no increase in the amount of the desired product. Parent cluster remained unreacted but further addition of BPK appeared to increase the amount of insoluble material (decomposition products) and the amount of $CH_3CCo_3(CO)_7dppe$. The solvent was removed and the residue chromatographed on silica gel plates. Elution with acetone/hexane (1:2) separated four major bands. The products were removed with acetone to yield: band 1, $CH_3CCo_3(CO)_9$ (33%, (0.01 g); band 2, $[CH_3CCo_3(CO)_8]_2dppe$ (41%); band 3, $CH_3CCo_3(CO)_7dppe$ (9%); band 4, $CH_3CCo_3(CO)_8dppe$ (8%).

Preparation of $CH_3CCo_3(CO)_7dppe$. $CH_3CCo_3(CO)_9$ (0.09 g, 0.2 mmol) and dppe (0.09 g, 0.23 mmol) were refluxed in 20 cm^3 of THF for ~5 min. The solvent was removed and the residue chromatographed on silica gel plates. Development in hexane/acetone (1:1) separated five bands. Band 1 gave $CH_3CCo_3(CO)_7dppe$ (0.13 g, 0.17 mmol, 83% yield). Other products were not characterized.

Reaction of $ClCCo_3(CO)_9$ with dppm. $ClCCo_3(CO)_9$ (0.09 g, 0.2 mmol) and dppm (0.08 g, 0.2 mmol) were refluxed in hexane until only a trace of starting cluster remained. Isolation of the major red brown product (chromatography) gave $ClCCo_3(CO)_7dppm$ (0.07 g, 0.09 mmol, 44% yield).

Reaction of $PhCCo_3(CO)_9$ with ttas. (a) Thermal Reaction. $PhCCo_3(CO)_9$ (0.10 g, 0.2 mmol) and ttas (0–12 g, 0.26 mmol) were refluxed in 20 cm^3 of THF. After 15 min, all parent cluster had been consumed and TLC showed a red-brown compound as the major product and a considerable amount of insoluble green material. The solution was cooled and filtered and the solvent removed under reduced pressure. The residue was dissolved in CH_2Cl_2, and the IR spectrum of this solution suggested that a trissubstituted cluster was the major product. The residue was chromatographed on silica gel plates and eluted with CH_2Cl_2/pentane (1:2). At least five brown and red-brown bands could be distinguished, but the material could not be removed from the gel with any common solvent, although the material was slightly soluble in CH_3CN and methanol. This indicated that decomposition of the product(s) had occurred, and the preparation was not persisted with.

(b) BPK Reaction. $PhCCo_3(CO)_9$ (0.05 g, 0.1 mmol) and ttas (0.09, 0.1 mmol) were dissolved in 10 cm^3 of dry, degassed THF. BPK was added dropwise to the stirred solution, and monitoring of the solution by TLC showed the slow formation of at least six products. After 30 min ~1 cm^3 of 2.5 × 10^{-3} mol dm^{-3} BPK had been added and a considerable amount of insoluble green material had precipitated from the solution although not all of the parent cluster had been consumed. Air was admitted to the flask, the solution rapidly became cloudy, and TLC analysis showed only small amounts of soluble material which was discarded.

Reaction of $PhCCo_3(CO)_9$ with tpme. (a) Thermal Reaction. $PhCCo_3(CO)_9$ (0.10 g, 0.2 mmol) and tpme (0.14 g, 0.22 mmol) were refluxed in 20 cm^3 of THF. After ~15 min all parent cluster had reacted and an orange compound was the major product. The solvent was removed under reduced pressure and the residue dissolved in a minimum of CH_2Cl_2. Bright orange microcrystalline material precipitated, and this was collected and identified as $PhCCo_3(CO)_6tpme$ by microanalysis.

(b) BPK Reaction. $PhCCo_3(CO)_9$ (0.10 g, 0.2 mmol) and tpme (0.24 g, 0.4 mmol) were dissolved in 10 cm^3 of dry degassed THF. After addition of several drops of BPK, analytical TLC of the solution (developed in hexane/acetone) showed unreacted cluster and five products (in order of decreasing R_f).

The green-brown product 1 formed initially in the greatest amount while the fourth and fifth brown products and insoluble

Table IV. Final Positional Parameters for $[PhCCo_3(CO)_8]_2dppe$

atom	x/a	y/b	z/c	atom	x/a	y/b	z/c
Co(1)	0.0170 (1)	0.1559 (1)	0.8100 (1)	C(16)	−0.2620 (3)	0.2177 (3)	0.2028 (3)
Co(2)	0.1833 (1)	0.2651 (1)	1.0369 (1)	C(17)	−0.1377 (3)	0.2525 (3)	0.3170 (3)
Co(3)	0.0874 (1)	0.3415 (0)	0.8196 (1)	C(18)	−0.1210 (3)	0.2900 (3)	0.4507 (3)
C_{ap}	0.1825 (5)	0.2285 (3)	0.8598 (5)	C(19)	0.0224 (4)	0.4909 (4)	0.5774 (5)
C(1)	0.2971 (3)	0.0905 (2)	0.8068 (4)	C(20)	0.0440 (6)	0.0330 (5)	0.8643 (6)
C(2)	0.4012 (3)	0.0603 (2)	0.7924 (4)	O(20)	0.0580 (5)	−0.0479 (4)	0.8930 (6)
C(3)	0.5007 (3)	0.1357 (2)	0.8137 (4)	C(21)	−0.0506 (5)	0.1027 (4)	0.6274 (7)
C(4)	0.4961 (3)	0.2414 (2)	0.8494 (4)	O(21)	−0.0958 (5)	0.0621 (3)	0.5120 (5)
C(5)	0.3921 (3)	0.2716 (2)	0.8639 (4)	C(22)	−0.1242 (7)	0.1787 (5)	0.8238 (9)
C(6)	0.2926 (3)	0.1961 (2)	0.8426 (4)	O(22)	−0.2131 (6)	0.1942 (5)	0.8354 (9)
P	0.0359 (1)	0.3542 (1)	0.5988 (1)	C(23)	0.2572 (7)	0.1599 (5)	1.1234 (6)
C(7)	0.2519 (4)	0.3987 (2)	0.5651 (4)	O(23)	0.3048 (6)	0.0951 (4)	1.1761 (5)
C(8)	0.3483 (4)	0.3724 (2)	0.5338 (4)	C(24)	0.3217 (7)	0.3632 (5)	1.1401 (7)
C(9)	0.3496 (4)	0.2682 (2)	0.4859 (4)	O(24)	0.4093 (6)	0.4244 (4)	1.2082 (6)
C(10)	0.2545 (4)	0.1904 (2)	0.4694 (4)	C(25)	0.0787 (7)	0.3041 (5)	1.1080 (7)
C(11)	0.1582 (4)	0.2168 (2)	0.5007 (4)	O(25)	0.0129 (6)	0.3296 (5)	1.1505 (6)
C(12)	0.1569 (4)	0.3209 (2)	0.5486 (4)	C(26)	0.2061 (6)	0.4530 (4)	0.8886 (6)
C(13)	−0.2285 (3)	0.2926 (3)	0.4702 (3)	O(26)	0.2818 (5)	0.5264 (4)	0.9326 (5)
C(14)	−0.3528 (3)	0.2578 (3)	0.3559 (3)	C(27)	−0.0426 (6)	0.3988 (4)	0.8308 (6)
C(15)	−0.3695 (3)	0.2203 (3)	0.2222 (3)	O(27)	−0.1227 (5)	0.4346 (4)	0.8426 (5)

(decomposition) material increased as more BPK was added. Air was admitted to the flask, the solvent removed, and the residue chromatographed on silica gel plates. The first three products were recovered and identified by IR (CH_2Cl_2) as follows: **1**, $[PhCCo_3(CO)_8]_n$tmpe (A); **2**, $PhCCo_3(CO)_7$tpme; **3**, $[PhCCo_3(CO)_8]_n$tpme (B).

(c) Bulk Electrolysis. Reactions of $PhCCo_3(CO)_9$ with tpme in CH_2Cl_2 and CH_3CN both resulted in nearly complete consumption of parent cluster. In acetone, a considerable amount of cluster remained unreacted and the current did not fall-off to the preelectrolysis value.

tpme (0.29 g, 0.45 mmol) was dissolved in 30 cm^3 of CH_2Cl_2 (0.1 mol dm^{-3} Bu_4NClO_4). After the preelectrolyzing solution was degassed, $PhCCo_3(CO)_9$ (0.15 g, 0.3 mmol) was added and solution electrolyzed at −0.55 V (vs. Ag/AgCl) until the current fell to the background value (~25 min). Monitoring of the solution during the reaction showed that the monosubstituted derivative A (product 1 above) was the initial major product and product **3** the minor product, while at the end of electrolysis, the bissubstituted derivative **2** was the major product. TLC also revealed at least five other products with (brown, yellow, and orange colored) R_f less than that of product **3**. These products were not isolated.

In CH_3CN, after decay of the electrolysis current, TLC analysis showed products **1** and **3** (monosubstituted derivatives) and only a very small amount of product **2**. The potential was incremented by −0.2 V, and a very slow reaction over several hours led to an increase in $PhCCo_3(CO)_7$tpme as well as to small amounts of yellow, brown, and orange products.

X-ray Data Collection and Reduction for $[PhCCo_3(CO)_8]_2$dppe. A sample of $[PhCCo_3(CO)_8]_2$dppe was prepared as outlined above and recrystallized from $CHCl_3$/ethanol. A black block-shaped crystal was used for data collection. Precession photography (Cu Kα radiation) indicated a triclinic unit cell, and the space group was confirmed as $P\bar{1}$ by the success of the structure refinement. Three-dimensional data were collected on a Nicolet $P\bar{3}$ four circle fully automatic computer-controlled diffractometer. The unit cell dimensions and orientation matrices were calculated from 25 accurately centred reflections. The data were processed and empirical absorption corrections were applied by using programs from the Shelxtl package.[25] Details of the crystal data collection and structure refinement are summarized in Table III.

The structure was solved by direct methods using the EEES procedures of program Shelx.[26] The E map revealed the positions of the three cobalt atoms and the phosphorus atom of the molecule which as a crystallographically imposed center of symmetry located midway between the methylene groups of the 1,2-bis(diphenylphosphino)ethane ligand. The remaining non-hydrogen atoms were found in subsequent difference Fourier, least-squares refinement cycles by using the program Shelx.[26] Refinement with isotropic thermal parameters for all heavy atoms resulted in $R = 0.0999$. The refinement was continued by using anisotropic temperature factors for the cobalt, phosphorus, apical carbon, carbonyl carbon and oxygen atoms, and the carbon atoms of the apical phenyl group.

All phenyl rings were treated as planar rigid groups (C–C = 1.40 Å) with isotropic temperature factors for the carbon atoms of the phenyl rings of the dppe ligand. The hydrogen atoms of the phenyl rings were included in calculated positions (C–H = 1.08 Å). A weighting scheme based on counting statistics was introduced, and final convergence gave $R = 0.0405$ and $R_w = 0.0448$ ($w = 2.4578/\sigma^2(F) + 0.000\,419F^2$).

A final difference Fourier synthesis showed four peaks in the range of 0.7–0.9 e $Å^{-3}$ in the vicinity of the metal atoms and the coordinated carbonyl groups with the remainder of the difference map having no peaks >0.45 e $Å^{-3}$. The relative weighting scheme appeared satisfactory since the minimized function showed little dependence on $|F_o|$ and $(\sin\theta)/\lambda$. No abnormal discrepancies were found between observed and calculated structure factors for those reflections not used in the refinement. Final atomic coordinates and other crystallographic data are given in Table IV and supplementary material.

Acknowledgment. A.J.D. thanks the University Grants Committee for the award of a post-graduate scholarship. We thank the University of Waikato for obtaining the ^{31}P and ^{13}C NMR spectra and Dr. R. G. Cunninghame for helpful discussions.

Registry No. **1**, 101011-65-8; **2**, 101011-56-7; BPK, 16592-08-8; $PhCCo_3(CO)_7$dppm(A), 101141-55-3; $PhCCo_3(CO)_6(dppm)_2$, 101011-58-9; $PhCCo_3(CO)_5(dppm)_2$, 101011-59-0; $PhCCo(CO)_4$dppm(B), 101141-56-4; $PhCCo_3(CO)_9$, 13682-03-6; $CH_3CCo_3(CO)_7$dppm(A), 101141-57-5; $CH_3CCo_3(CO)_7$dppm(B), 101141-58-6; $CH_3CCo_3(CO)_5(dppm)_2$, 101011-60-3; $CH_3CCo_3(CO)_9$, 13682-04-7; $[PhCCo_3(CO)_8]$.2dppe, 101011-54-5; $PhCCo_3(CO)_3$dppe, 101011-61-4; $[CH_3CCo_3(CO)_8]_2$dppe, 101031-40-7; $CH_3CCo_3(CO)_4$dppe(A), 101011-62-5; $CH_3CCo_3(CO)_8$dppe, 101011-63-6; $ClCCo_3(CO)_9$, 13682-02-5; $CcCCo_3(CO)_7$dppm, 101011-64-7; $PhCCo_3(CO)_6$tpme, 101011-55-6; benzophenone, 119-61-9.

Supplementary Material Available: Deposited crystallographic data for $[PhCCo_3(CO)_8]_2$dppe includes thermal parameters of non-hydrogen atoms (Table S1), positional parameters for calculated hydrogen atoms (Table S2), F_o and F_c structure factor tables (Table S3), selected least-squares planes (Table S4), and bond lengths and angles in the calculated phenyl rings (Table S5) (21 pages). Ordering information is given on any current masthead page.

(25) Sheldrick, G. M. Shelxtl, "An Integrated System for Solving, Refining and Displaying Crystal Structures from Diffraction Data", University of Gottinjen, 1981.

(26) Sheldrick, G. M. Shelx-76, "Program for Crystal Structure Determination", University of Cambridge, 1976.